TECHNICAL RESEARCH REPORT

SYSTEMS RESEARCH CENTER

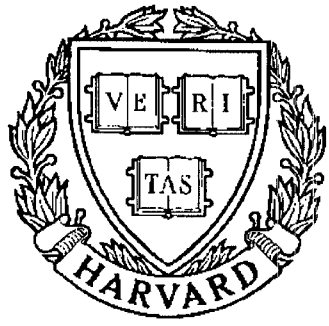

Supported by the National Science Foundation Engineering Research Center Program (NSFD CD 8803012), Industry and the University

Bifurcation Analysis of Nonuniform Flow Patterns in Axial-Flow Gas Compressors

by R.A. Adomaitis and E.H. Abed

TR 92-121

Bifurcation Analysis of Nonuniform Flow Patterns in Axial-Flow Gas Compressors

Raymond A. Adomaitis and Eyad H. Abed
Institute for Systems Research
University of Maryland
College Park, MD 20742

Manuscript date: 3 December 1992
Submitted to the proceedings of the 1st World Congress
of Nonlinear Analysts, August 1992, Tampa

Abstract

We study the transition from steady, spatially uniform-flow to nonuniform and time-dependent gas axial velocity profiles in an axial flow compression system. Local bifurcation analysis of the uniform-flow solution reveals a series of bifurcations to traveling waves of different mode number as a function of throttle opening. The number of bifurcating modes is found to depend on the gas viscosity parameter, an effect introduced in this work. Using the local approximations of the bifurcating solutions as starting points of our numerical analysis, we uncover a complicated scenario of secondary bifurcations ultimately resulting in parameter ranges where locally asymptotically stable stalled-flow solutions of different mode number coexist.

Introduction

A common feature observed in a variety of compressor configurations is the loss of stability of the steady, spatially-uniform gas flow when the system is operated near peak pressure-rise conditions. The resulting post instability behavior leads to decreased operating performance of the compressor and even to mechanical damage of the compression system. Thus, there is a great incentive to understand the complicated sequence of flow instabilities that mark the end of uniform flow so that the system stability margin can be accurately quantified.

In the most general terms, there are two fundamentally different post-instability equilibria: surging flow and rotating stall (Greitzer, 1976). Compressor *surge* occurs when the plenum gas pressure exceeds the compressor pressure rise and so low frequency (in time) oscillations of the mean gas flow rate develop. *Rotating stall* is a local aerodynamic phenomenon that occurs when the gas passing through the rotor disengages

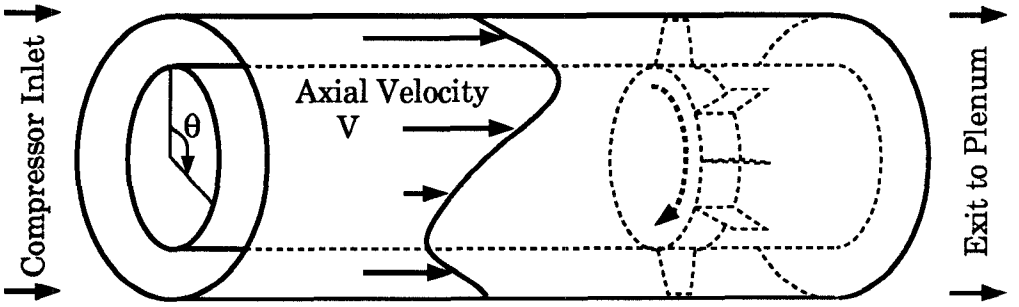

Figure 1 A schematic of the compressor geometry.

from the blade surface, reducing the local gas flow rate (Day, 1991a). In this case, the bulk gas flow remains constant in time, but flow measurements taken along the circumferential coordinate (θ of Fig. 1) of the compressor rotor will reveal spatial variations of the local gas flow. This means the local gas velocity takes the form of a traveling wave, rotating about the compressor annulus.

There is an inadequate understanding of the transitions to these undesirable operating conditions. Coexistence of multiple attractors, subcritical bifurcations of the post-instability equilibria and periodic solutions, and global bifurcations of the periodic solutions lead to complicated dynamics in the phase space and intricate sequences of transitions with changing parameters (Liaw *et al.*, 1991; Adomaitis *et al.*, 1992). The introduction of computational dynamics and bifurcation techniques to the analysis of these systems gives a rational framework with which to study and organize the observed behavior, and most importantly, to give a rigorous definition to the compressor stability margin (McCaughan, 1989a,b).

This work begins with a modification to the 2-dimensional partial differential equation model of Moore and Greitzer (1986) to account for viscous dissipation of energy in the compressor. Linearized stability analysis of the uniform flow solution is performed, followed by a weakly nonlinear analysis of the bifurcating stalled-flow solutions. The local nonlinear analysis shows, for our particular system, that low mode number stalled-flow solutions are born in *subcritical bifurcations* while higher mode number solutions are born in *supercritical* bifurcations. This analysis also gives us a starting point for the numerical computation and continuation of the stalled-flow solutions. A wealth of secondary bifurcations along the stalled flow branches is revealed, including symmetry-breaking and bifurcations to modulated traveling waves. The most important aspect of the secondary bifurcations is that they give rise to ranges of operating conditions where locally asymptotically stable stalled-flow patterns of different mode number coexist.

Modification of the Moore-Greitzer Model

The model used is based on Moore and Greitzer's (1986) model, but a term which accounts for momentum transfer in the compressor section by viscous transport is also included. A local momentum balance describing the two-dimensional flow in the

Parameter	*Value*	*Description*
α	1/3.5	fluid inertial term
l_c	8.0	overall compressor length
m	1.75	exit duct length factor
H	0.18	compressor characteristic height factor
w	0.25	compressor characteristic width factor
f_0	0.3	compressor characteristic vertical offset
μ	0.01	fluid viscosity

Table 1 Compressor parameters used in this work.

compressor and its associated ducting (Fig. 1) gives the partial differential equation:

$$\Delta_p = f(V + v_0) - l_C \frac{dV}{d\tau} - m\frac{\partial}{\partial \tau}\int_{-\infty}^{0} v d\eta - \frac{1}{2\alpha}\left[2\frac{\partial v_0}{\partial \tau} + \frac{\partial v_0}{\partial \theta} - \mu\frac{\partial^2 v_0}{\partial \theta^2}\right]. \qquad (1)$$

Note that our notation differs considerably from the original notation of Moore and Greitzer: V denotes the annulus-averaged (mean) gas axial velocity; v_0 is the axial velocity perturbation evaluated at $\eta = 0$ (the inlet face of the compressor); Δ_p is the plenum-to-atmosphere pressure rise; η, θ are the axial and angular coordinates, respectively; and μ is the gas viscosity.

The compressor pressure rise $f(V_{loc})$ is particular to each compressor and is obtained from experiments in the stable operating range and estimated in the nonuniform-flow range. Following Moore and Greitzer, we use a cubic equation in axial velocity

$$f(V_{loc}) = f_0 + H\left[1 + \frac{3}{2}\left(\frac{V_{loc}}{w} - 1\right) - \frac{1}{2}\left(\frac{V_{loc}}{w} - 1\right)^3\right]$$

where $V_{loc} = V + v_0$ (the total local axial flow) and the characteristic parameters used throughout this work are given in Table 1. If the momentum balance (1) is averaged over the circumferential coordinate, we find

$$l_C \frac{dV}{d\tau} + \Delta_p(\tau) = \frac{1}{2\pi}\int_0^{2\pi} f d\theta \qquad (2)$$

which can be thought of as determining the amplitude of the zeroth-order Fourier mode, and so (2) determines the transient behavior of the mean flow (V). If there are no spatial variations of gas density and pressure in the plenum, an overall material balance on the gas over the plenum gives:

$$l_C \frac{d\Delta_p}{d\tau} = \frac{1}{4B^2}\left[V(\tau) - F^{-1}(\Delta_p)\right] \qquad (3)$$

where the throttle characteristic is given by the orifice equation $F^{-1}(\Delta_p) = \gamma\sqrt{\Delta_p}$. The parameter γ is proportional to the throttle opening.

Uniform Flow Dynamics

If there are no spatial perturbations in the flow field (so $v_0 = 0$), the local momentum balance PDE reduces to (2) which can be further simplified to

$$l_C \frac{dV}{d\tau} + \Delta_p = f(V). \tag{4}$$

This means the dynamics (but not necessarily the true stability, as we shall see) in the uniform flow subspace is governed entirely by (3-4). Steady, uniform flow solutions can be understood physically by the requirement that the pressure rise through the compressor ($\Delta_p = f(V)$) must equal the pressure drop through the throttle opening ($\Delta_p = F(V)$). Thus, the solutions are determined by the intersections of the graphs of the compressor and throttle characteristics.

Since the position of the throttle characteristic is parameterized by the throttle opening parameter γ, we can construct bifurcations diagrams illustrating the behavior of the steady flow and time periodic solutions to (3-4) born at the surge Hopf bifurcation points[1] as a function of throttle opening. A representative bifurcation diagram is given in Fig. 2. Notice that since the stability characteristics *in the full space* are shown in this diagram, some of the transitions cannot be accounted for solely by the two-ODE model. This illustrates the necessity for analysis of the full ODE/PDE model.

Linearized Stability With Respect to Spatial Perturbations

Substituting the annulus-averaged momentum balance (2) into the local momentum balance (1) and linearizing at $V = \hat{V}$ and $v_0 = 0$, we find

$$0 = \frac{df(\hat{V})}{dV} v_0 - m\frac{\partial}{\partial\tau}\int_{-\infty}^{0} v\,d\eta - \frac{1}{2\alpha}\left[2\frac{\partial v_0}{\partial\tau} + \frac{\partial v_0}{\partial\theta} - \mu\frac{\partial^2 v_0}{\partial\theta^2}\right]. \tag{5}$$

Solutions are linear combinations of functions which are periodic in the circumferential coordinate θ, satisfy $v_0 = 0$ at the inlet duct entrance (at $\eta \to -\infty$), and satisfy the continuity condition (since we assume potential flow in the ducting). Thus, substituting $v_n = z_n \exp(\lambda_n\tau + n\eta + in\theta)$ into (5) and solving for the eigenvalues λ_n, we obtain

$$\left[\frac{m}{n} + \frac{1}{\alpha}\right]\lambda_n = \frac{df(\hat{V})}{dV} - \mu\frac{n^2}{2\alpha} \pm i\frac{n}{2\alpha}. \tag{6}$$

[1] If we linearize the system at a steady, uniform-flow solution point (so $V = \hat{V}$, $\Delta_p = \hat{\Delta}_p$, and $v_0 = 0$), the linearized ODEs decouple from the PDE (there are no v_0 terms after linearization) and so their eigenvalues are the sole determinant of the location of the surge point.

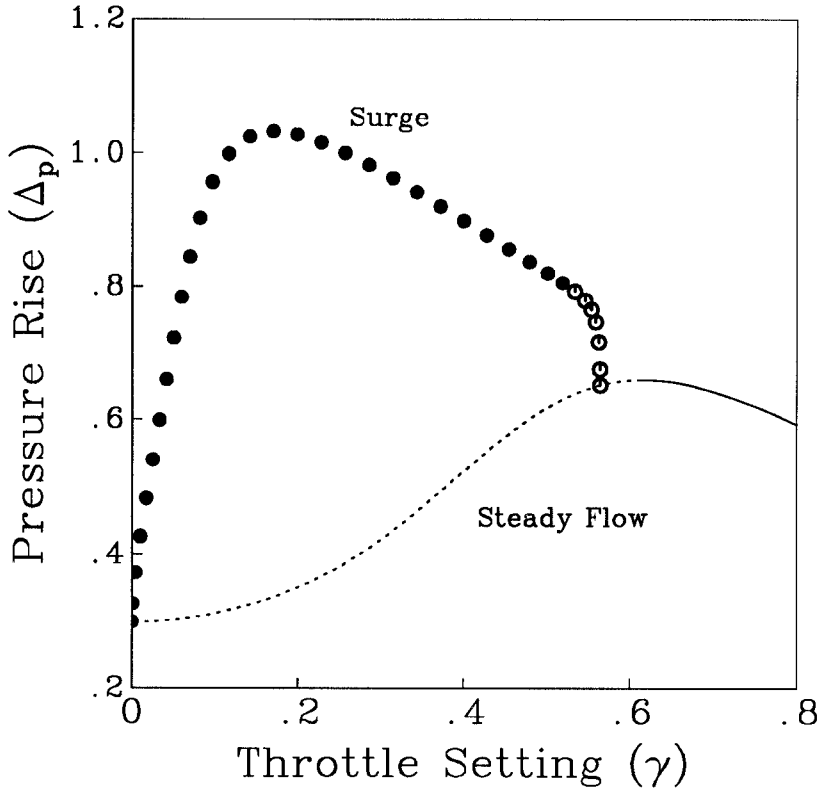

Figure 2 Steady and time-periodic uniform flow solutions for $B = 0.5$. Stability is represented in the full (two Fourier modes) space. Dashed line represents unstable steady flow, solid line stable steady flow, o unstable surge flow, and • stable surge flow.

This expression can be given some physical "feel" by considering its behavior for very small (positive) μ. For all μ and all mode numbers n, the real part of the eigenvalue expression will be negative for compressor characteristic segments where the derivative of the characteristic with respect to the mean flow V is negative (see the right-most portion of the uniform-flow solution branch in Fig. 3). As the throttle is closed (moving left on the solution branch), the local maximum is crossed and so the derivative changes sign. This means, for small μ and the first Fourier mode ($n = 1$), the real part of the eigenvalue vanishes at a point just to the left of the peak. Since this point will move farther down (to the left) the uniform-flow branch as the viscosity parameter increases, we see, true to what we should expect, that viscous effects tend to damp out spatial perturbations. Similar arguments can be made for the higher mode (n) bifurcation points shown in Fig. 3.

The Bifurcating Traveling Waves—Local Analysis

The rotating stall equilibria are spatial waves of local axial velocity, some of which rotate at a constant speed around the annulus. Rather than computing these traveling wave solutions as limit cycles in the Fourier coefficient space, a more efficient method is to introduce a rotating coordinate frame $\theta \mapsto \theta + c\tau$ so that the amplitude coefficients of

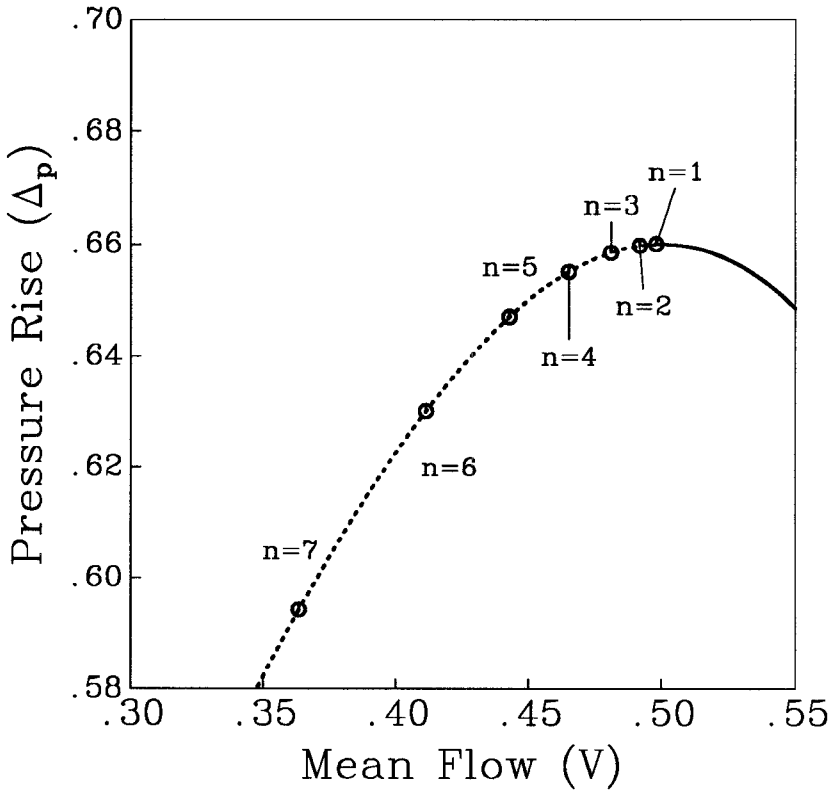

Figure 3 A portion of the uniform-flow solution branch in the uniform-flow phase space (parameterized by throttle opening γ) for the viscosity parameter value $\mu = 0.01$. Circles indicate bifurcation points corresponding to different mode numbers n.

the traveling waves can be found as fixed points. Making this coordinate change affects the PDE (1) only:

$$\Delta_p = f(V + v_0) - l_C \frac{dV}{d\tau} - m \int_{-\infty}^{0} \left[c\frac{\partial v}{\partial \theta} + \frac{\partial v}{\partial \tau} \right] d\eta$$

$$-\frac{1}{2\alpha}\left[2c\frac{\partial v_0}{\partial \theta} + 2\frac{\partial v_0}{\partial \tau} + \frac{\partial v_0}{\partial \theta} - \mu\frac{\partial^2 v_0}{\partial \theta^2}\right]. \tag{7}$$

If we approximate v by the eigenfunction associated with the eigenvalue λ_n

$$v = \exp(n\eta)[a_n \cos(n\theta) + b_n \sin(n\theta)] \tag{8}$$

(and so $v_0 = a_n \cos(n\theta) + a_n \sin(n\theta)$), substitute (8) into (7) to form the residual, use Galerkin's method to determine the amplitude coefficients, and constrain the Fourier coefficients by the relationship

$$A_n^2 = a_n^2 + b_n^2,$$

we obtain the greatly simplified, third-order set of ODEs:

$$\frac{m\alpha+n}{n\alpha}\frac{dA_n}{d\tau} = \left[\frac{3HV}{2w^3}(2w-V) - \frac{\mu n^2}{2\alpha}\right]A_n - \frac{3H}{8w^3}A_n^3;$$
$$l_C\frac{dV}{d\tau} = -\Delta_p + f_0 + \frac{HV^2}{2w^3}(3w-V) + \frac{3H}{4w^3}(w-V)A_n^2; \qquad (9a,b,c)$$
$$l_C\frac{d\Delta_p}{d\tau} = \frac{1}{4B^2}\left[V - \gamma\sqrt{\Delta_p}\right],$$

a set ordinary differential equations closely related to the third-order model of Moore and Greitzer (1986).

A number of features of the steady, stalled-flow solutions can be computed by hand for this severely truncated approximation of the stalled-flow profile. The wave speed c is computed from the requirement that if the coordinates rotate in Fourier space at the same speed as the traveling wave, the eigenvalues at the stall bifurcation points will cross the imaginary axis *on* the real axis. It can be shown (see Adomaitis, 1992 for details) that this condition gives

$$c = \frac{-n}{2(\alpha m+n)} \qquad (10)$$

(c.f. Eq. (57) of Moore and Greitzer). The amplitude of the bifurcating traveling wave comes from the steady-state form of (9a) with $A_n \neq 0$:

$$A_n^2 = \beta\left[\frac{df}{dV} - \mu\frac{n^2}{2\alpha}\right] \qquad \text{where} \qquad \beta = \frac{8w^3}{3H}. \qquad (11)$$

The steady mean flow V can now be computed from (9b)

$$\Delta_p = \left(\frac{V}{\gamma}\right)^2 = \frac{1}{2\pi}\int_0^{2\pi} f\,d\theta = f_0 + \frac{HV^2}{2w^3}(3w-V) + \frac{3H}{4w^3}(w-V)A_n^2. \qquad (12)$$

For $A_n \neq 0$, the mean gas velocity V of the stalled-flow solutions are defined by the cubic polynomial in V:

$$f_0 - \left(\frac{V}{\gamma}\right)^2 - \frac{15HV^2}{2w^2} + \frac{5HV^3}{2w^3} + \frac{6HV}{w} + (V-w)\frac{\mu n^2}{\alpha} = 0. \qquad (13)$$

We must be careful in interpreting solutions to (13), since some of the roots, when substituted back into (11), will give $A_n^2 < 0$, clearly an impossible physical result.

In the limit of $B \to 0$ (small plenum size), equations (9) reduce to two since we can write $\Delta_p = (V/\gamma)^2$. Linearizing at some mean flow $\hat{V}$ and mode amplitude $\hat{A}_n$ gives

$$\frac{m\alpha+n}{n\alpha}\frac{dA_n}{d\tau} = \left[\frac{df}{dV} - \frac{\mu n^2}{2\alpha} + \frac{3}{8}\frac{d^3f}{dV^3}\hat{A}_n^2\right](A_n - \hat{A}_n) + \left[\hat{A}_n\frac{d^2f}{dV^2}\right](V-\hat{V});$$
$$l_C\frac{dV}{d\tau} = \left[\frac{1}{2}\frac{d^2f}{dV^2}\hat{A}_n\right](A_n - \hat{A}_n) + \left[\frac{df}{dV} - \frac{2V}{\gamma^2} + \frac{1}{4}\frac{d^3f}{dV^3}\hat{A}_n^2\right](V-\hat{V}). \qquad (14a,b)$$

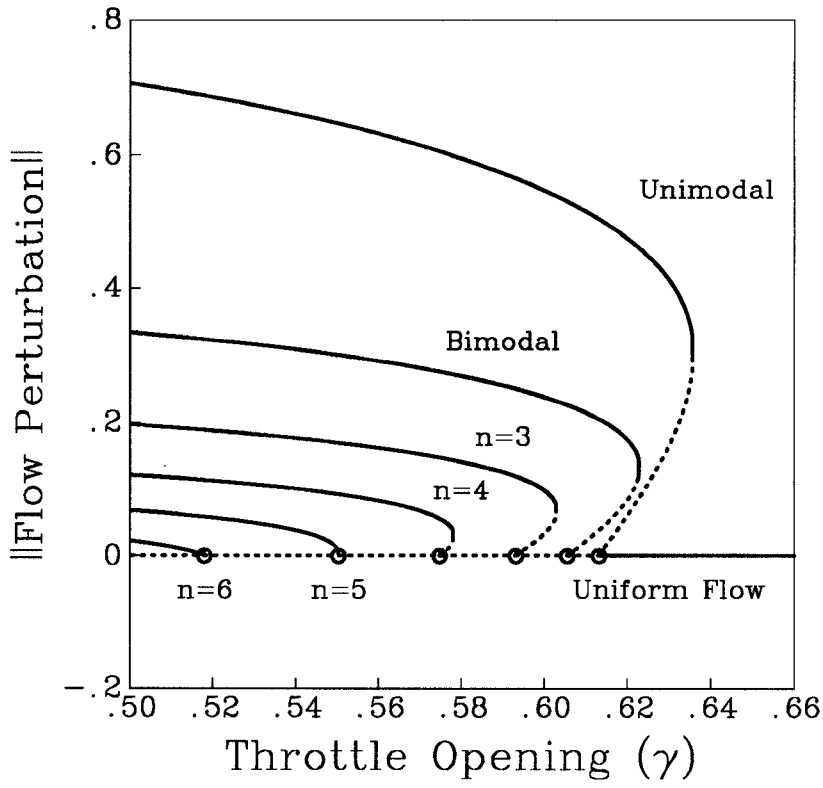

Figure 4 Bifurcating stalled-flow solutions computed via local methods. Stability assignments (solid curves = stable, dashed curves = unstable) correspond to the eigenvalues of (14), and so *do not necessarily apply in the full space*. Compressor characteristic inflection point is at $\gamma \approx 0.361$ and the local peak is at $\gamma \approx .615$. The $n = 7$ branch falls outside the range shown.

The bifurcation diagram shown in Fig. 4 is computed using (13) to compute the mean flow V of the bifurcating branches as a function of γ which can be used in (11) to obtain the amplitude of the stall mode. Proof that the low-mode stalled-flow solutions are born in subcritical bifurcations and the high-mode number solutions are born in supercritical bifurcations can be found in Adomaitis (1992)—these facts should be apparent from the numerical evidence presented in Fig. 4. The stability of the bifurcating solution is determined by the eigenvalues of (14), although it is important to note that the stability determined in this manner reflects stability with respect to perturbations of mode number equal to that of the bifurcating solution. Stability in the full Fourier space is discussed in the following section.

The Bifurcating Traveling Waves—Numerical Results

The gas axial velocity perturbation is given by

$$v = \sum_{n=1}^{N} \exp(n\eta)[a_n \cos(n\theta) + b_n \sin(n\theta)]$$

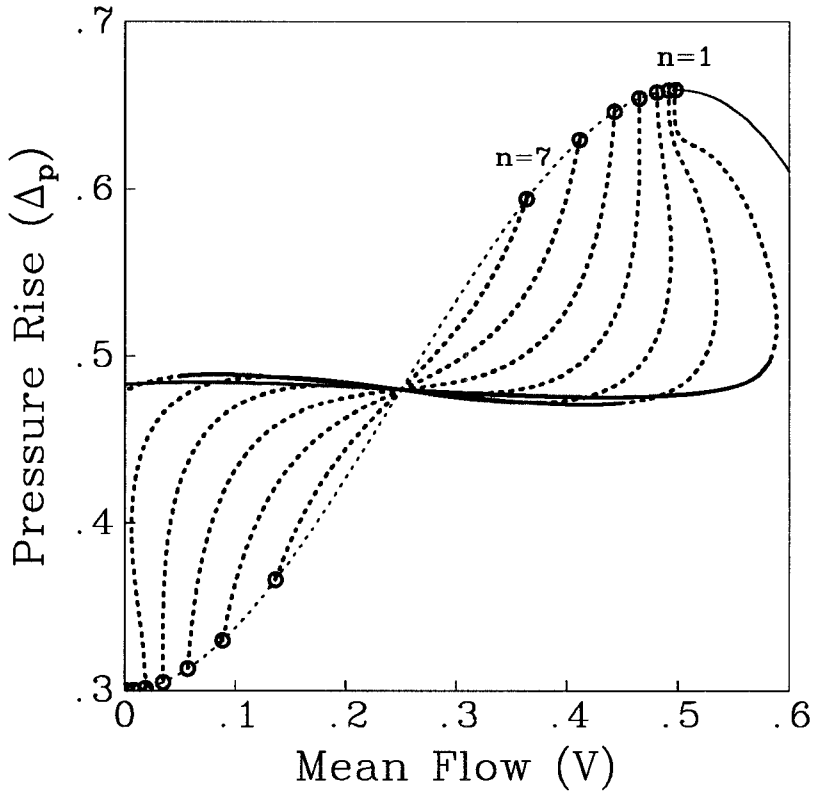

Figure 5 Stalled-flow solution branches computed with 24–mode discretizations (c.f. Fig. 4.23 of Lavrich, 1988).

and so, as before, the axial velocity profile at the inlet guide vanes is denoted v_0 (at $\eta = 0$). Substituting the Fourier expansion into the local momentum balance PDE in a rotating coordinate frame (7) and using Galerkin's method to determine the amplitude coefficients, the $\cos(n\theta)$ moment gives, after some rearranging,

$$\left\{\frac{m}{n}+\frac{1}{\alpha}\right\}\dot{a}_n = \frac{1}{\pi}\int_0^{2\pi} f\cos(n\theta)d\theta - \frac{\mu n^2}{2\alpha}a_n - \left(cm+\frac{cn}{\alpha}+\frac{n}{2\alpha}\right)b_n$$

and the $\sin(n\theta)$ moment gives

$$\left\{\frac{m}{n}+\frac{1}{\alpha}\right\}\dot{b}_n = \frac{1}{\pi}\int_0^{2\pi} f\sin(n\theta)d\theta - \frac{\mu n^2}{2\alpha}b_n + \left(cm+\frac{cn}{\alpha}+\frac{n}{2\alpha}\right)a_n$$

along with the ODEs (3-4). One of the advantages of using the cubic compressor characteristic is that the integrals can be evaluated explicitly. These results are discussed in detail in Adomaitis (1992).

Thus, we obtain a large set of ordinary differential equations in time describing the dynamics of the Fourier mode amplitude coefficients that can be analyzed with

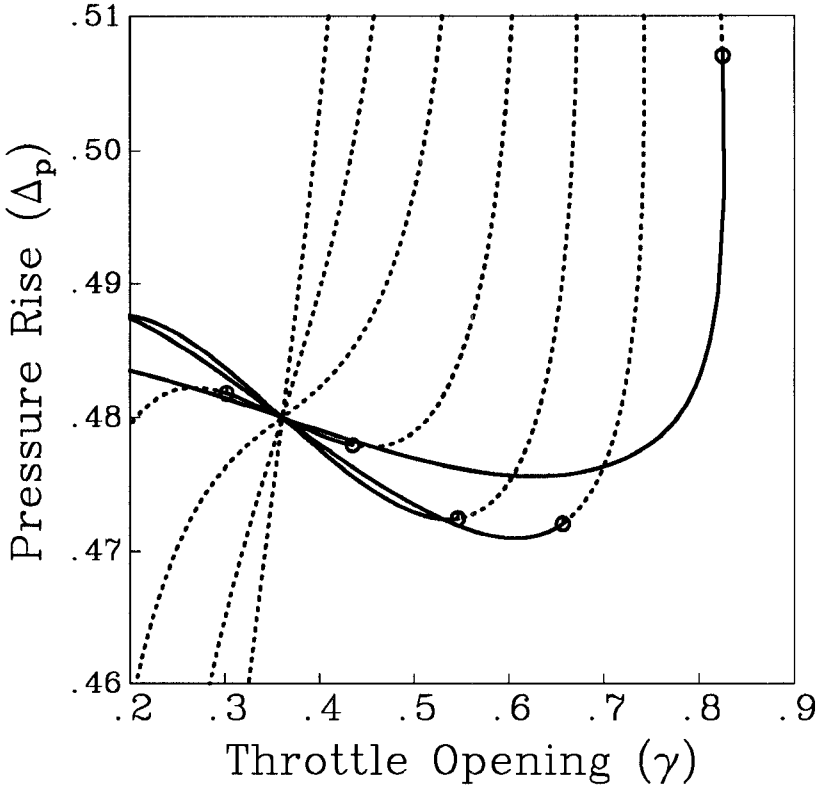

Figure 6 Solution branches of Fig. 5 plotted as a function of throttle opening. The stability limits of the stable sections of the bimodal and higher solution branches are marked by bifurcations to modulated traveling waves.

standard numerical bifurcation analysis techniques. We use the local bifurcation analysis discussed in the previous section for determining the initial points on the solution branches corresponding to the different stalled-flow modes and follow these branches with a predictor-corrector continuation technique, similar to the one discussed in Doedel (1981). Representative results are shown in Figs. 5 and 6.

There are a number of secondary bifurcations that take place along the stalled-flow solution branches. All of the equilibrium solutions born in subcritical bifurcations go through a saddle-node bifurcation; in the unimodal case, this results in a long segment of stable, stalled-flow solution banch (see Fig. 7 for a representative flow profile). The bimodal and all other n-modal stalled-flow solutions born off the uniform-flow solution branch have the property that if the solution is shifted by $2\pi/n$, the plot of axial velocity will fall back on top of itself. Branches of solutions which do not possess this symmetry are born off of the n-modal (with $n \geq 2$) solution branches shown in Figs. 5 and 6. Finally, bifurcations to modulated traveling waves result in locally asymptotically stable segments of the bimodal, trimodal, and 4-cell stalled-flow branches. No stable ranges along the higher-mode solution branches were found, although we suspect this would not be the case for smaller values of the viscosity parameter (μ). By plotting these solutions as a function of the throttle opening parameter, we see that there is a range of operating

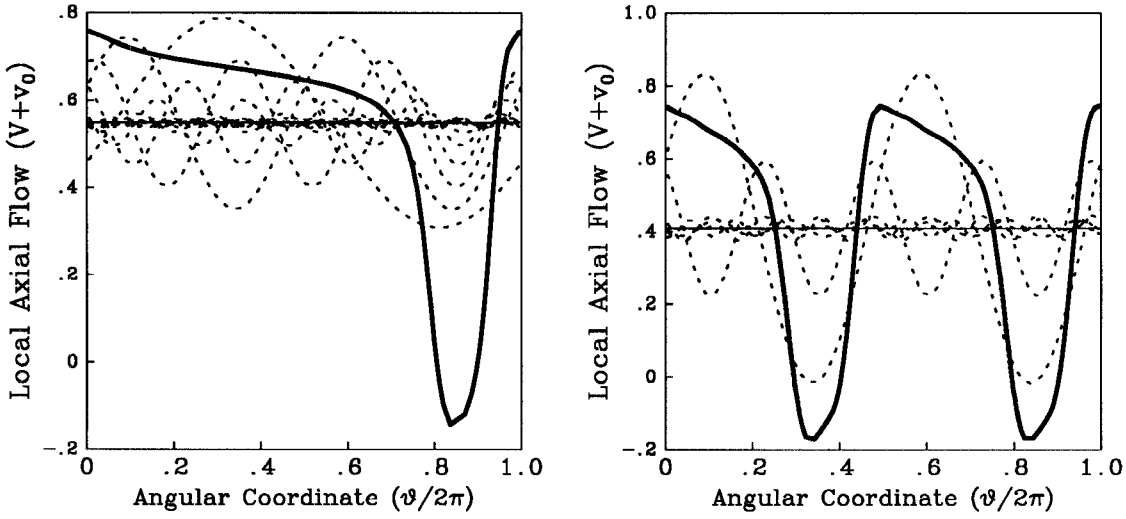

Figure 7 Representative axial flow profiles along the unimodal (left) and bimodal (right) branches. Both flow profiles are locally asymptotically stable. Dashed curves are the contributions of the different Fourier modes, solid denotes the sum.

conditions where different mode stall cells which are locally asymptotically stable coexit (Fig. 6). This corroborates with the experimental observation of Lavrich (1988).

Conclusions

We have used a combination of local (analytical) and numerical bifurcation analysis techniques to study the transitions from spatially-uniform, time-invariant gas flow profiles in axial flow compressors to those with spatial structure. The primary contribution of this work is the numerical study of the sequence of bifurcations resposible for ranges of operating conditions where rotating stall cells of different mode number coexist and are locally asymptotically stable.

This type of analysis is well suited for accurate computation of the instability margin. It is also useful for evaluating control schemes designed for active instability suppression. Most work in this area is focused on experimental systems (Paduano *et al.*, 1991; Day, 1991b) for stall control, or pure simulation of controllers designed primarily for surge supression (Badmus *et al.*, 1991; Hosney *et al.*, 1991). We feel the bifurcation-theoretic approach will be useful in evaluating the global dynamical behavior of control systems for active instability suppression.

References

Abed, E. H., P. K. Houpt, and W. M. Hosny (1990). Bifurcation analysis of surge and rotating stall in axial flow compressors. *Proc. 1990 Amer. Contr. Conf.*, San Diego, 2239-2246.

Adomaitis, R. A. (1992). Rotating Stall in Axial Flow Compressors. Part I – Stall Pattern Bifurcation Analysis., in preparation.

Adomaitis, R. A., D. -C. Liaw, and E. H. Abed (1992). Nonlinear dynamics of axial-flow compressors: A parametric study. *ASME J. Dyn. Syst. Measurement and Control*, under revision.

Badmus, O. O., C. N. Nett, and F. J. Schork (1991). An integrated, full-range surge control/rotating stall avoidance compressor control system. *Proc. 1991 Amer. Contr. Conf.*, Boston.

Day, I. J. (1991a). Stall inception in axial flow compressors. *Proc. 1991 ASME Gas Turbine Conf.*, Orlando.

Day, I. J. (1991b). Active supression of rotating stall and surge in axial compressors. *Proc. 1991 ASME Gas Turbine Conf.*, Orlando.

Doedel, E. J. (1981). AUTO: A program for the automatic bifurcation analysis of autonomous systems. *Cong. Num.*, **30**, 265-284.

Greitzer, E. M. (1976). Surge and rotating stall in axial flow compressors Part I: Theoretical compression system model. *ASME J. of Engineering for Power*, **112**, 190-198.

Hosny, W. M., L. Leventhal, and W. G. Steenken (1991). Active stabilization of multistage axial-compressor aerodynamic system instabilities. *Proc. 1991 ASME Gas Turbine Conf.*, Orlando.

Lavrich, P. L. (1988). Time resolved measurements of rotating stall in axial flow compressors. *MIT Gas Turbine Laboratory Report # 194*

Liaw, D. -C., R. A. Adomaitis, and E. H. Abed (1991). Two-parameter bifurcation analysis of axial flow compressor dynamics. *Proc. 1991 Amer. Contr. Conf.*, Boston.

Moore, F. K. and E. M. Greitzer (1986). A theory of post-stall transients in axial compression systems: Part I—Development of equations. *ASME J. of Engineering for Gas Turbines and Power* **108**, 68-76.

McCaughan, F. E. (1989a). Application of bifurcation theory to axial flow compressor instability. *ASME J. of Turbomachinery* **111**, 426-433.

McCaughan, F. E. (1989b). Numerical results for axial flow compressor instability. *ASME J. of Turbomachinery* **111**, 434-441.

Paduano, J., A. H. Epstein, L. Valavani, J. P. Longley, E. M. Greitzer, and G. R. Guenette (1991). Active control of rotating stall in a low speed axial compressor. *Proc. 1991 ASME Gas Turbine Conf.*, Orlando.